Bioelectromagnetics 42:159–172 (2021)

Effects of 2600 MHz Radiofrequency Radiation in Brain Tissue of Male Wistar Rats and Neuroprotective Effects of Melatonin

Kevser Delen [1]*, Bahriye Sırav [1], Sinem Oruç [1], Cemile M. Seymen [2], Dilek Kuzay [3], Korkut Yeğin [4] and Gülnur Take Kaplanoğlu [2]

[1]Department of Biophysics, Faculty of Medicine, Gazi University, Ankara, Turkey
[2]Department of Histology and Embryology Faculty of Medicine, Gazi University, Ankara, Turkey
[3]Department of Physiology, Kırşehir Ahi Evran University, Kırşehir, Turkey
[4]Department of Electrical and Electronics Engineering, Ege University, Izmir, Turkey

The debate on the biological effects of radiofrequency radiation (RFR) still continues due to differences in the design of studies (frequency, power density, specific absorption rate [SAR], exposure duration, cell, tissue, or animal type). The current study aimed to investigate the effects of 2,600 MHz RFR and melatonin on brain tissue biochemistry and histology of male rats. Thirty-six rats were divided into six groups randomly: cage-control, sham, RFR, melatonin, sham melatonin, and RFR melatonin. In RFR groups, animals were exposed to 2,600 MHz RFR for 30 days (30 min/day, 5 days/week) and the melatonin group animals were subcutaneously injected with melatonin (7 days/week, 10 mg/kg/day) for 30 days. SAR in brain gray matter was calculated as 0.44 and 0.295 W/kg for 1 and 10 g averaging, respectively. RFR exposure decreased the GSH, GSH-Px, and SOD levels and increased the MPO, MDA, and NOx levels ($P < 0.005$) significantly. RFR exposure also led to an increase in structural deformation and apoptosis in the brain tissue. This study revealed that exogenous high-dose melatonin could reduce these adverse effects of RFR. Limiting RFR exposure as much as possible is recommended, and taking daily melatonin supplements may be beneficial. Bioelectromagnetics. 2021;42:159–172. © 2021 Bioelectromagnetics Society

Keywords: apoptosis; brain tissue; melatonin; oxidative stress; radiofrequency radiation

INTRODUCTION

On the basis of the studies associating the increased risk of glioma with cellular phone use, the International Agency for Research on Cancer (IARC) declared radiofrequency radiation (RFR) as a carcinogen (possibly carcinogenic to humans) in 2011 [Baan et al., 2011]. Since the brain is a vital tissue and under close exposure to RFR, it is essential to examine the effects of RFR on brain tissue. Due to its low antioxidant enzyme activity and high oxygen consumption, brain tissue is more vulnerable to oxidative damage [Motawi et al., 2014]. Studies about the effects of RFR exposure on the nervous system demonstrated that neuropsychiatric complaints, such as headaches, dizziness, depressive symptoms, memory changes, and sleep disorders were more common among individuals living around base stations [Abdel-Rassoul et al., 2007], and RFR exposure caused changes in electroencephalography activity [Lustenberger et al., 2013] and blood-brain barrier permittivity [Sirav and Seyhan, 2016]. Also, RFR on neuronal activity may be related to regional blood flow changes in brain tissue due to RFR exposure [Aalto et al., 2006].

On the contrary, studies about RFR have conflicting results. It is hard to reach a common conclusion obtained from different studies due to the differences in study designs, such as RFR frequency,

Grant sponsor: Gazi University Scientific Research Projects Coordination Unit; grant number: 01/2018-05.

Conflicts of interest: None.

*Correspondence to: Kevser Delen, Department of Biophysics, Faculty of Medicine, Gazi University, 06560 Ankara, Turkey. Email: kevserdelen@gazi.edu.tr

Received for review 14 August 2020; Accepted 20 December 2020

DOI:10.1002/bem.22318
Published online 13 January 2021 in Wiley Online Library (wileyonlinelibrary.com).

modulation, specific absorption rate (SAR), exposure duration, cell, or animal type. Therefore, further studies about RFR have great importance in terms of enlightening the effects of RFR. Several studies reported that RFR caused an increase in apoptosis, oxidative stress, DNA damage, and inflammation in the brain tissue [Salford et al., 2003; Megha et al., 2015; Chauhan et al., 2017; Alkis et al., 2019], while others showed no effect [Sakuma et al., 2006; Joubert et al., 2007]. Induction of oxidative stress can be one of the most important reasons for the biological effects of RFR. Oxidative stress occurs as a result of the disruption of the balance between free oxygen radicals and antioxidants in cells and tissues. It was suggested that oxidative effects of RFR depended on some factors, such as increasing free radicals, peroxidation activation, DNA damage, and change in antioxidant enzyme activities [Yakymenko et al., 2016]. In some studies, RFR exposure and antioxidant agent were applied together to prevent oxidative damage secondary to RFR, and oxidative damage could be prevented [Köylü et al., 2006; Kerman and Senol, 2012; Koç et al., 2014].

Melatonin is a potent antioxidant secreted mainly from the pineal gland. Melatonin plays a role in many receptor-dependent and independent processes. Receptor-dependent functions are the regulation of circadian rhythm, sleep, and cancer inhibition. Receptor-independent processes occur due to the ability of melatonin to perform free radical detoxification [Reiter et al., 2014]. Melatonin's amphiphilic structure allows easier passage of it through the blood-brain barrier and cell membrane than most other antioxidants [Hardeland, 2009]. Melatonin has a circadian rhythm that is mainly regulated by light, and peak levels of serum melatonin occur at night. Bothorel et al. [2002] reported that melatonin administration in Wistar rats caused an increase in the nocturnal peak of endogenous melatonin. Pan et al. [2006] found that the antioxidant effect of melatonin was dose-dependent. Based on this finding, we preferred to use a high dose (10 mg/kg/day) of melatonin in this study.

Astrocytes, a subtype of glial cells, are important for maintaining brain homeostasis. In mature astrocytes, glial fibrillary acidic protein (GFAP) is the primary intermediate filament protein, and GFAP immunohistochemistry is a method to visualize astrocytes [Halliday et al., 1996; Middeldorp and Hol, 2011]. It was reported that diseases or damage of the brain tissue caused an increase in the synthesis of GFAP from astrocytes [Schmidt-Kastner et al., 1993]. Further evaluation of immunohistochemistry analysis can be carried out by using H-score. The H-score method can be used to evaluate the extent of nuclear immunoreactivity semiquantitatively, which can be calculated by multiplying the staining intensity by the stained cell percentage [John et al., 2009].

In this study, the aim was to examine the degenerative (histology, oxidative damage, and apoptosis) effects of 2,600 MHz RFR exposure (30 days, 5 days/week, 30 min/day), and to analyze the possible protective effects of high-dose melatonin (30 days, 7 days/week, 10 mg/kg/day) in male Wistar rats' brain tissue.

MATERIALS AND METHODS

Animals

Male Wistar albino rats (250–300 g) were used. Animals were housed under standard conditions (12 h light/12 h dark cycle and the temperature was 22 ± 2 °C). Animals were given tap water as drinking water and fed ad libitum.

Study Groups

Following one week of adaptation, 36 rats were divided into six groups randomly as follows: Cage-Control Group ($n = 6$): No experimental application was performed. Sham Group ($n = 6$): Same procedure was carried out to the RFR exposure group, but without energizing the RFR system. RFR Group ($n = 6$): 2,600 MHz RFR exposure was performed for 30 days (30 min, 5 days/week). Melatonin Group ($n = 6$): Cage-controls with daily melatonin injection (10 mg/kg, subcutaneous [sc] injection) group; melatonin injection was administered for 30 days (7 days/week). Sham Melatonin Group ($n = 6$): Sham exposure and daily melatonin injection were performed. RFR melatonin Group ($n = 6$): RFR exposure and daily melatonin injection were performed.

Exposure System and Design

The 2,600 MHz RFR exposures were carried out by using a signal generator (frequency range: 9 kHz–3.2 GHz, Model SMBV100A; Rohde & Schwarz, Munich, Germany) with the 3GPP-FDD setting, and the average level of the signal was set to 20 dBm (100 mW). Exposures were applied with a horn antenna (frequency range: 400 MHz–6 GHz, Model 3164-03; ESCO Technologies, Cedar Park, TX). A similar experimental procedure was performed on sham group animals, but the RFR system was not activated. RFR and sham exposures were carried out at the same time every day. During exposure, rats were placed in plastic cages ($34 \times 24 \times 13$ cm), three animals in one cage and exposures were performed by placing the horn antenna on the plastic cage. Using

broadband radiofrequency (RF) survey meter (Model EMR-300; L3 Communications, Pfullingen, Germany) with the appropriate probe, electric (E) field measurements were performed. E field values inside the plastic cages were measured at five different points and the mean E field value was 21.74 V/m. Background E field value was 0.88 V/m. To calculate the SAR values, the experimental setup with three rats positioned with a 120° angle under the horn antenna was replicated in a simulation environment using Computer Simulation Technology (CST), which is a 3D electromagnetic field solver based on finite-integration technique. Whole-body SARs were calculated as 0.616 W/kg for 1 g average and 0.297 W/kg for a 10 g average using IEEE/IEC 62704-1 method. SAR in brain gray matter was calculated as 0.44 and 0.295 W/kg for 1 and 10 g averaging, respectively. Rat voxel model and SAR distributions for sagittal plane cuts are given in Figure 1.

Melatonin Treatment

One hundred milligrams of melatonin (Lot: 4O2HH-RH; Tokyo Chemical Industry, Tokyo, Japan) was dissolved in 100 µl (100% pure) alcohol, and 9,900 µl phosphate-buffered saline (PBS) (pH = 7.4) was added. Melatonin solution was prepared daily and subcutaneously injected (10 mg/kg/day). Melatonin treatments were performed at the same time every day (5 pm) for 30 days.

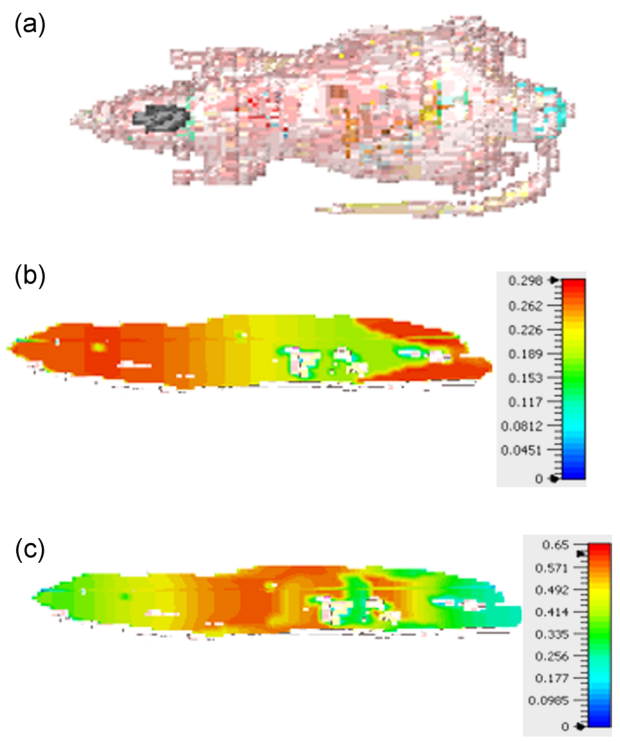

Fig. 1. Specific absorption rate (SAR) computations at 2,600 MHz, (**a**) rat voxel model with brain highlighted in a dark color, (**b**) sagittal cut whole-body SAR distribution for 10 g average, (**c**) sagittal cut whole-body SAR distribution for 1 g average.

Brain Tissue Preparation

At the end of the experimental procedure, the rats were decapitated under deep anesthesia by intramuscular injection with ketamine (45 mg/kg) and xylazine (5 mg/kg). Oxidative damage parameters were analyzed with one hemisphere of the brain tissue and histological examinations were carried out at the other hemisphere.

Oxidative Analysis

Brain tissue samples were frozen in liquid nitrogen following decapitation and kept at −80 °C until analyzed. After the homogenization (PBS, pH 7.2–7.4) step, samples were centrifuged at 2,000–3,000 rpm for 20 min and the supernatants were removed. Following the manufacturer's instructions, the levels MDA, NOx, MPO, GSH, SOD, and GSH-Px in the supernatant were measured by using ELISA kits (Shanghai Sunred Biological Technology, Shanghai, China). Samples absorbance was measured at 450 nm. Results were expressed as ng/ml for SOD, GSH-Px, and MPO, as nmol/ml for MDA, as µmol/g for Nox, and as mg/L for GSH.

Immunohistochemical and Histochemical Analysis

The fixation of brain tissue samples of all groups was done in 10% neutral formaldehyde for 72 h. At the end of the routine histological follow-up procedure, cross-sections of tissues were cut at 4 µm and hematoxylin-eosin was performed. To perform the immunohistochemical analysis by using citrate buffer (pH 6.0), the heat-induced antigen retrieval procedure was performed. The activity of the endogenous peroxidase was inhibited by 3% H_2O_2. A serum-blocking solution was used for 10 min to stabilize the epitopes (Lot: 1754084 A; LifeTech, Waltham, MA). Incubations with anti-GFAP antibody ([bs-0199R]; 1:100 [with PBS]; overnight at +4 °C) of the sections were performed. After this step, tissues were incubated at room temperature for 15 min with biotinylated secondary antibody. Washing with PBS was done between steps. 3,3′-Diaminobenzidine (DAB, Lot: 38703; ScyTek, West Logan, UT) was used for visualization of antibody-binding sites. As a next step, counterstaining with Harris hematoxylin was done. Slides were washed in water and alcohol and cleared in xylene, and covered with balsam. GFAP staining

density and intensity was assessed by a photo-light microscope (Model DM4000B; Leica Microsystems, Wetzlar, Germany), a plus camera (Model Leica DFC280; Leica Microsystems, Cambridge, UK), and a software program (LAS; Leica Microsystems). GFAP staining intensity was evaluated by using a semi-quantitative scoring system. This immunohistochemistry (IHC) scoring was: no staining as (0), weak staining as (1), weak to moderate staining as (2), moderate staining as (3), moderate to strong staining as (4), and strong staining as (5). Evaluation of the IHC scoring was carried out by two expert histologists separately. The H-score calculation was done by using the following formula: H-score = ΣPi $(i + 1)$, where Pi is the percentage of the stained cells and i is GFAP staining intensity.

Terminal deoxynucleotidyl transferase (TdT)-mediated dUTP nick-end labeling (TUNEL) Analysis

Using the in situ Apoptosis Detection Kit (cat no. S7101, ApopTag Plus Peroxidase; Chemicon, Temecula, CA), the TUNEL assay was performed. After the Proteinase-K step, endogenous peroxidase was blocked by using 3% hydrogen peroxide. TdT enzyme was applied at 37 °C for 1 h. Following the incubation of the cells in the stop/wash buffer (10 min), reactions were stopped. The next step was proceeding with anti-digoxigenin conjugate for 30 min. Peroxidase substrate DAB (cat. no. 00-2020; Invitrogen, Carlsbad, CA) was applied to the sections for detecting TUNEL-positive cells (counterstaining in Harris hematoxylin was performed for 1 min). Six areas (one central and five peripheral) of each coverslip were scanned. TUNEL index calculation was done by assessing the TUNEL-positive nuclei percentage among the total number of 100 nuclei counted.

Statistical Analysis

Results of biochemical and apoptotic index analyses were compared with Kruskal–Wallis and Mann–Whitney U tests by using SPSS 15.0 (SPSS; LEAD Technologies, Chicago, IL). The results are given as mean values. $P < 0.05$ was considered statistically significant.

RESULTS

Oxidative Effects of RFR in Brain Tissue

While RFR exposure caused a statistically significant decrease in GSH, GSH-Px, and SOD levels, it caused a significant increase in MPO, MDA, and NOx levels ($P < 0.005$). No significant difference was found between (1) Cage-Control and Sham groups, (2) Melatonin and Sham Melatonin groups, (3) Cage-Control and Melatonin groups, (4) Sham and Sham Melatonin groups. It was observed that melatonin administration decreased the oxidative effects of RFR ($P < 0.005$) (Table 1).

Effects of RFR on Brain Tissue Histology

The pia mater and other substantia grisea (cortex) tissues were observed in normal structure with neurons, supporting neuroglial cells, and blood vessels in the cage-control, sham, sham melatonin, and melatonin groups (Figs. 2 and 3A, B, E, and F). Cornu Ammonis 3 and 1 (CA3 and CA1) regions of the hippocampus of these groups were also observed in normal appearance with different neuron types, neuroglia cells, and blood vessels (Figs. 2 and 3C, D, G, and H). Those neurons are thought to have higher metabolic activity compared with other neurons (Fig. 3C, D, G, and H).

TABLE 1. Mean Values of MDA, NO, GSH, GSH-Px, MPO, and SOD Levels in Brain Tissue

Group	MDA (nmol/ml)	NOx (μmol/g)	GSH (mg/L)	GSH-Px (ng/ml)	MPO (ng/ml)	SOD (ng/ml)
Cage-control	5.83	9.03	36.76	7.23	0.70	5.60
Sham	5.85	8.98	36.88	7.16	0.70	5.78
RFR	12.58[a, b, c]	12.51[a, b, c]	11.18[a, b, c]	2.96[a, b, c]	1.71[a, b, c]	2.08[a, b, c]
Melatonin	5.86	8.90	37.55	7.26	0.69	6.1
Sham melatonin	5.98	8.60	37.13	7.35	0.70	5.81
RFR melatonin	8.01[a, d, e, f]	9.95[a, d, e, f]	30.48[a, d, e, f]	5.53[a, d, e, f]	0.85[a, d, e, f]	4.85[d, e, g]

[a]Significantly different from Cage-Control group ($P < 0.005$).
[b]Significantly different from Sham group ($P < 0.005$).
[c]Significantly different from RFR Melatonin group ($P < 0.005$).
[d]Significantly different from RFR group ($P < 0.005$).
[e]Significantly different from Melatonin ($P < 0.005$).
[f]Significantly different from Sham Melatonin group ($P < 0.005$).
[g]Significantly different from Sham Melatonin and RFR Melatonin groups ($P < 0.05$).

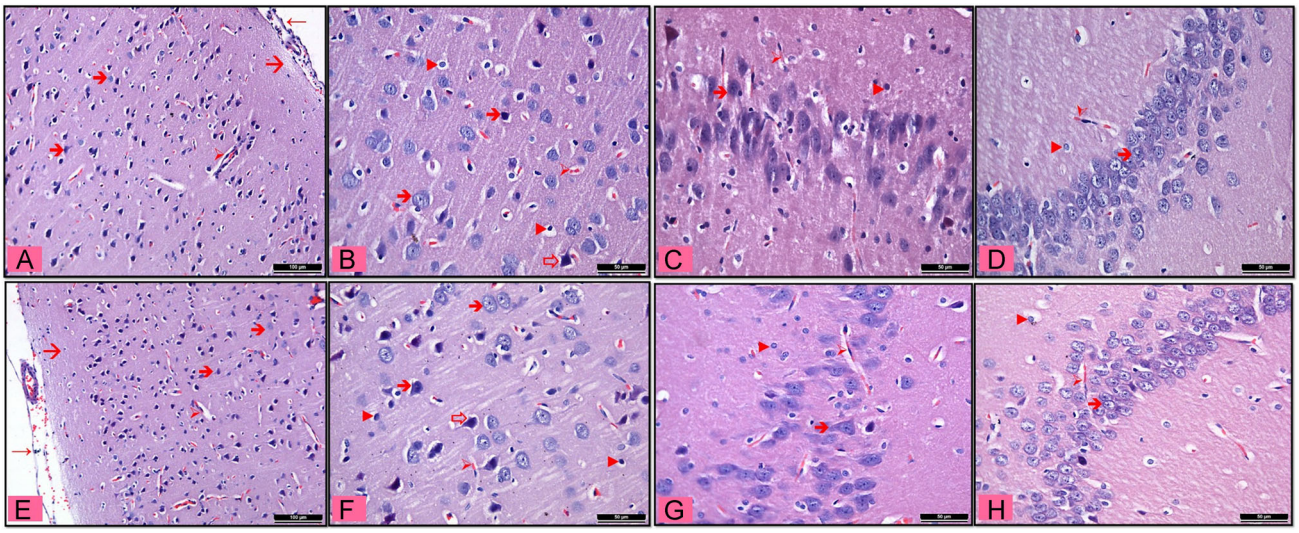

Fig. 2. Brain tissue sections of the Control and Sham Control groups. Control (**A**, **B**, Cortex; **C**, CA3; **D**, CA1], Sham Control (**E**, **F**, Cortex; **G**, CA3; **H**, CA1]. →, pia mater; →, molecular layer; ➔, neuron; ►, neuroglia cells; ➢, blood vessels; ⇨, pyramidal neuron (hematoxylin-eosin ×200 [**A** and **E**] ×400 [others]).

In the RFR group, the pia mater and molecular layer were observed in a normal structure. Additionally, dilated blood vessels, pyramidal neurons with abnormal morphology, and apoptotic neurons were observed in the cortex (Fig. 4A and B). In the hippocampus CA3 region of the RFR group, it was distinguished that neurons lost their normal course and showed random placement, neurons with abnormal morphology continued to appear, and also the number of neurons decreased semiquantitatively and the number of astrocytes increased (Fig. 4C). Dilated blood vessels and edema were observed around the neuroglia cells in the CA1 region of the hippocampus (Fig. 4D). In the RFR melatonin group, the pia mater and molecular layer were seen in normal structure, while dilated blood vessels were still present. Pyramidal neurons with abnormal morphology were still found in the cortex (Fig. 4E and F). The CA3

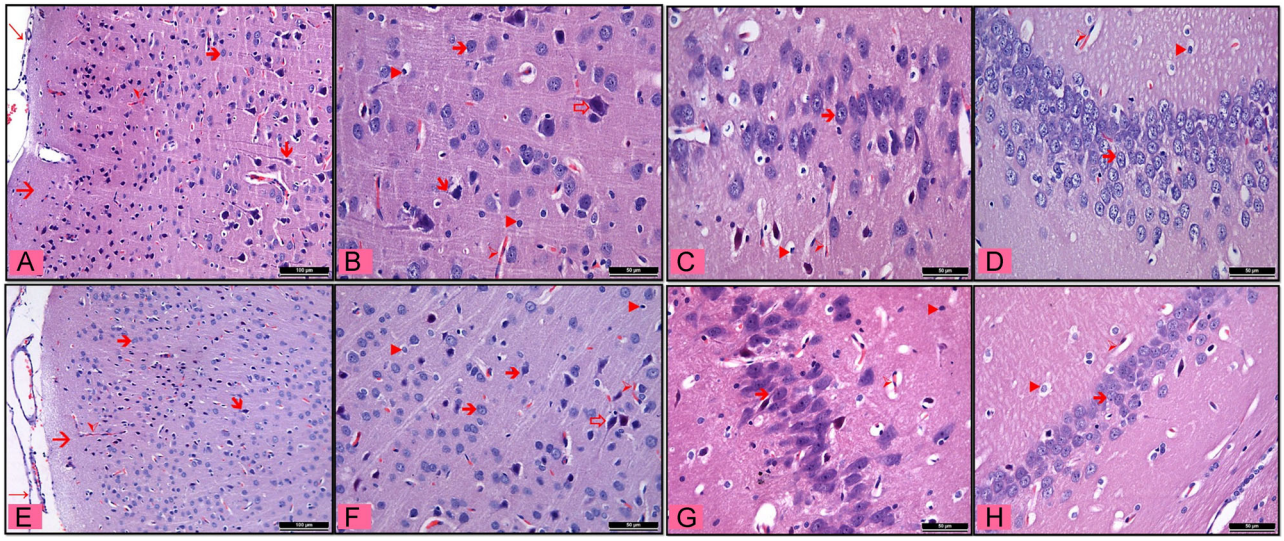

Fig. 3. Brain tissue sections of the Sham Melatonin and Melatonin groups. Sham Melatonin (**A**, **B**, Cortex; **C**, CA3; **D**, CA1), Melatonin (**E**, **F**, Cortex; **G**, CA3; **H**, CA1]. →, pia mater; →, molecular layer; ➔, neuron; ►, neuroglia cells; ➢, blood vessels; ⇨, pyramidal neuron (hematoxylin-eosin ×200 [**A** and **E**] ×400 [others]).

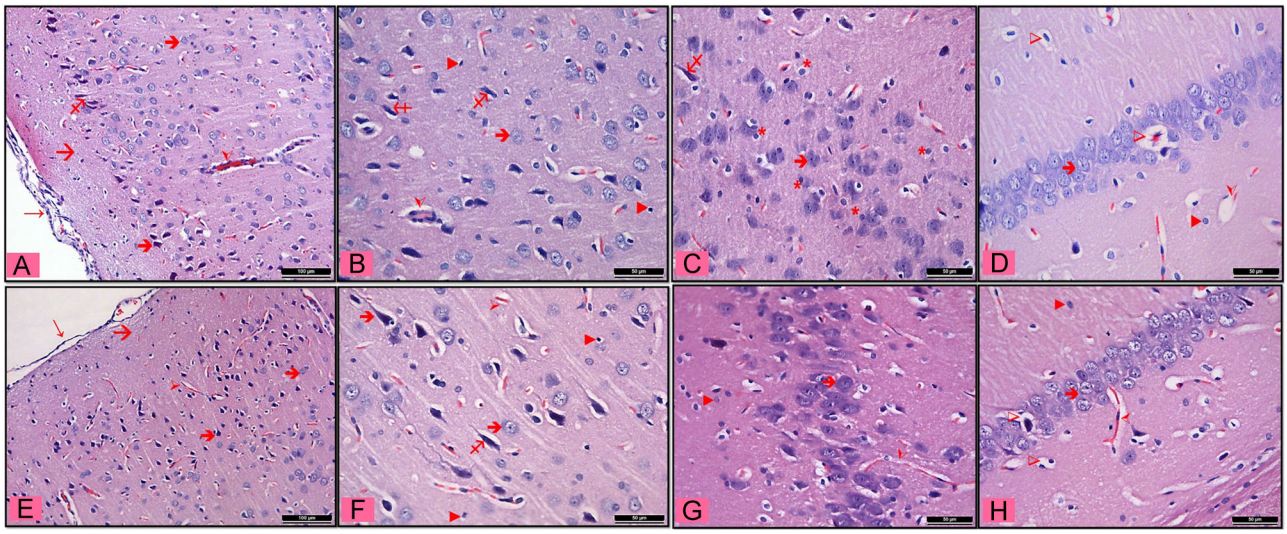

Fig. 4. Brain tissue sections of the RFR and RFR Melatonin groups. RFR (**A**, **B**, cortex; **C**, CA3; **D**, CA1), RFR melatonin (**E**, **F**, cortex; **G**, CA3; **H**, CA1]. →, pia mater; →, molecular layer; ➔, neuron; ►, neuroglia cells; ➢, blood vessels; ⇨, pyramidal neuron; ➢, dilated blood vessels; ⇗, pyramidal neuron with abnormal morphology; *, astrocyte; Δ, edema (hematoxylin-eosin ×200 [**A** and **E**] ×400 [others]). RFR = radiofrequency radiation.

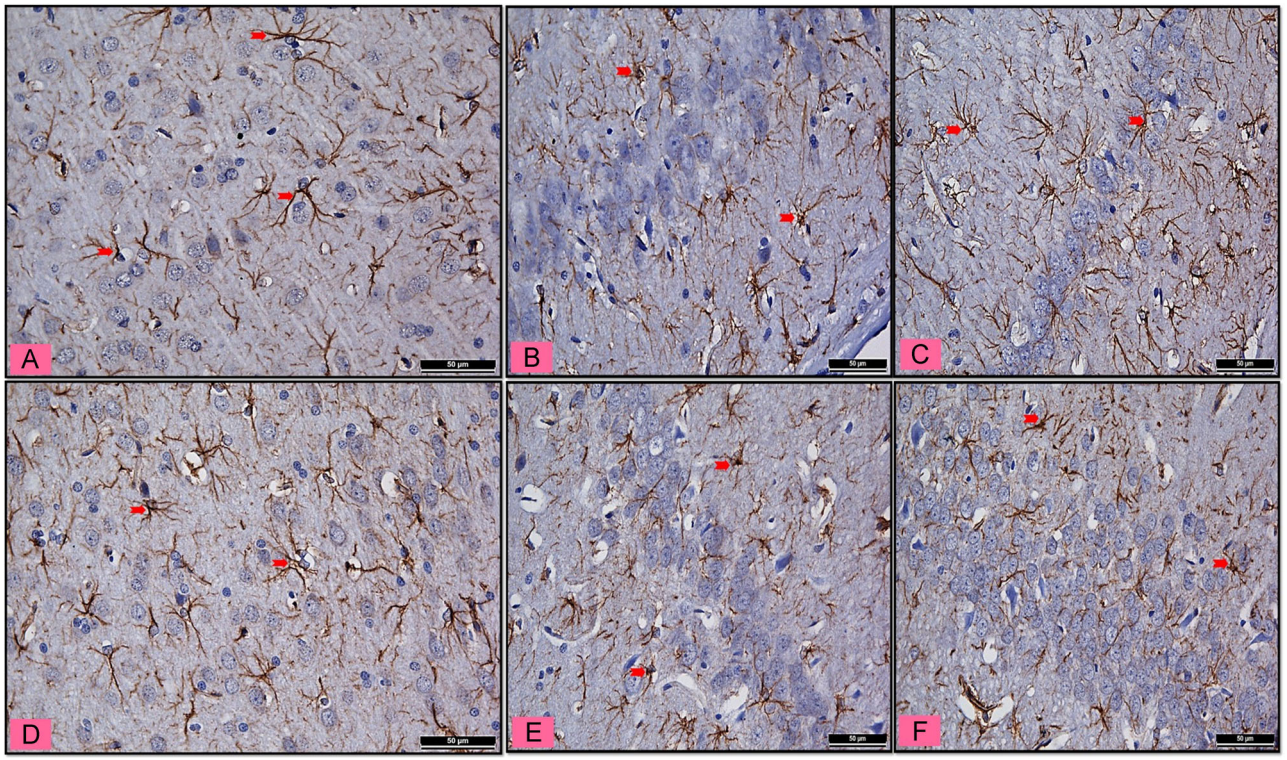

Fig. 5. GFAP immunoreactivity of the Control and Sham Control groups. Control (**A**, Cortex; **B**, CA3; **C**, CA1), Sham Control (**D**, Cortex, **E**, CA3; **F**, CA1). ➠, Astrocytes with GFAP immunoreactivity (immunoperoxidase-hematoxylin ×400). GFAP = glial fibrillary acidic protein.

region of the hippocampus was similar to the cage-control groups (Fig. 4G); vascular dilatation, edema around the neurons, and neuroglia cells were observed in the CA1 region of the hippocampus, but the structure was generally similar to the cage-control groups (Fig. 4H).

Effects of RFR on Brain Tissue Immunoreactivity

In the cortex and hippocampal CA3 and CA1 regions of the cage-control, sham, sham melatonin, and melatonin groups, strong GFAP immunoreactivity was observed in some astrocytes (Figs. 5 and 6). In the cortex and hippocampal CA3 and CA1 regions of the RFR group, strong GFAP immunoreactivity was observed in a greater number of astrocytes than the other groups. Extremely strong GFAP immunoreactivity was seen in the cortical astrocytes compared with the hippocampal regions. It was also noted that GFAP-positive astrocytes observed in the CA3 region of the hippocampus were more intense compared with the other regions. Astrocytes are responsible for regenerating by replacing damaged neurons. Therefore, this finding was confirmed with the semiquantitively decreased neurons finding that was observed in the same region of hematoxylin-eosin staining (Fig. 7). In the RFR melatonin group, the intensity and immunoreactivity of GFAP were similar compared to the cage-control group (Fig. 8). According to statistical findings, GFAP immunoreactivity was found significantly higher in the RFR group than cage-control, sham, and RFR melatonin groups. Additionally, significantly higher H-score values were observed in the RFR melatonin group than cage-control, melatonin, and sham melatonin groups ($P < 0.05$) (Fig. 9).

Apoptotic Effects of RFR in Brain Tissue

TUNEL staining is a method to detect apoptosis and can be used to distinguish apoptosis from necrosis [Sharma et al., 2013]. A small number of TUNEL-positive neurons and neuroglia cells were observed in the cortex and hippocampal regions of the cage-control, control, melatonin, and sham melatonin groups (Figs. 10 and 11). However, in the RFR group, a large number of TUNEL-positive neurons and neuroglia cells were seen in both cortex and hippocampus. It was observed that the number of TUNEL-positive cells was higher than the hippocampus. Apoptosis was seen in both neuron and neuroglial cells in the cortex, but it was noted that the

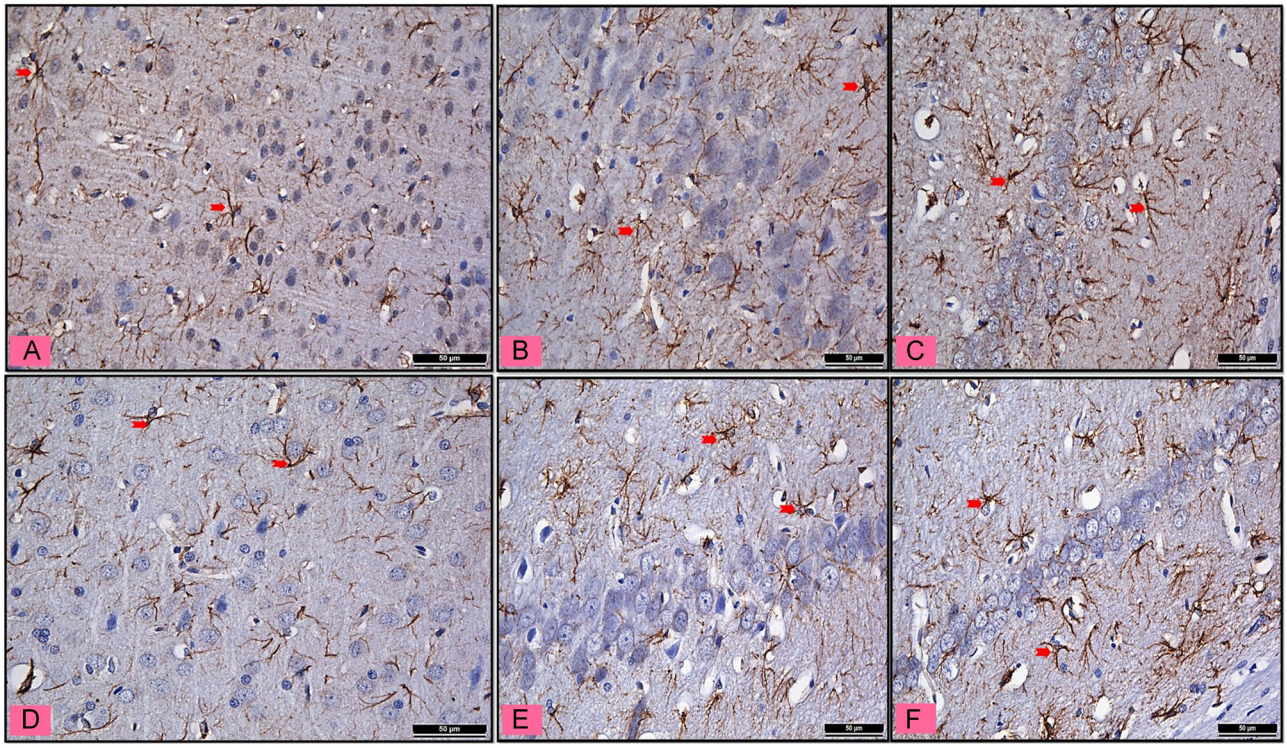

Fig. 6. GFAP immunoreactivity of the Sham Melatonin and Melatonin groups. Sham Melatonin (**A**, cortex; **B**, CA3; **C**, CA1), Melatonin (**D**, cortex, **E**, CA3; **F**, CA1). ➡, Astrocytes with GFAP immunoreactivity (immunoperoxidase-hematoxylin ×400). GFAP = glial fibrillary acidic protein.

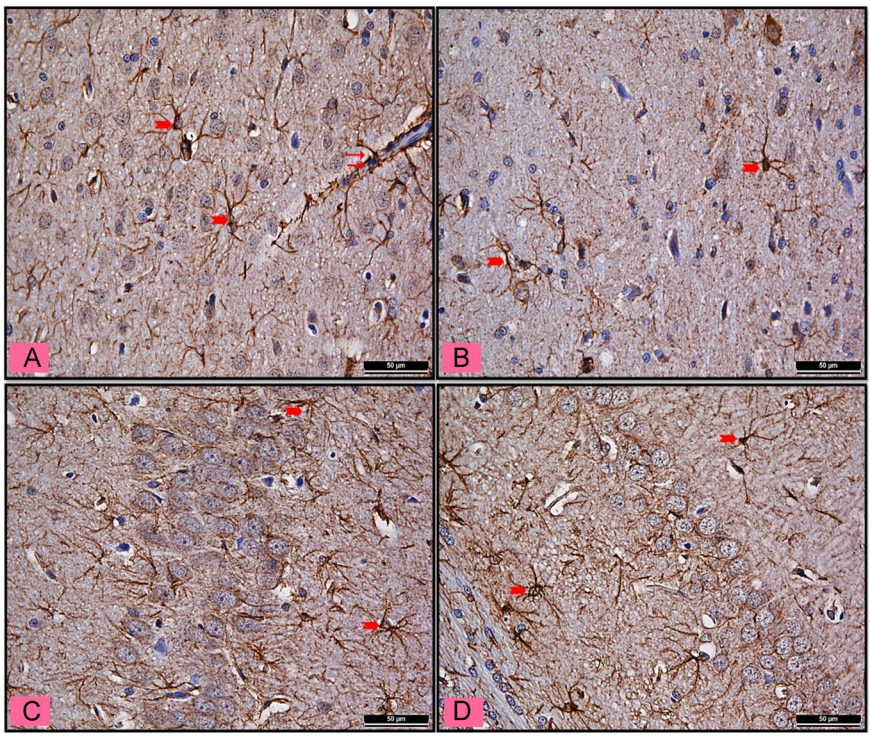

Fig. 7. GFAP immunoreactivity of the RFR group. RFR (**A**, **B**, cortex; **C**, CA3; **D**, CA1). ➡, Astrocytes with GFAP immunoreactivity; ⇉, Astrocytes and their extensions with GFAP immunoreactivity around the blood vessels (immunoperoxidase-hematoxylin ×400). GFAP = glial fibrillary acidic protein; RFR = radiofrequency radiation.

most apoptotic cells in the hippocampus were seen through neuroglial cells (Fig. 12A and B). In the RFR melatonin group, TUNEL-positive cells were detected both in the cortex and in the hippocampus, mostly in neuroglial cells but also in neurons. TUNEL-positive cell density was not the same as the RFR group but was not lower than the cage-control groups (Fig. 12C and D). It was observed that apoptotic index values were significantly higher in the RFR group than cage-control and sham ($P < 0.005$) groups. In the RFR melatonin group, apoptotic index values were found to be significantly lower than the RFR group ($P < 0.05$). Also, in the RFR melatonin group, apoptotic index values were found to be significantly higher than

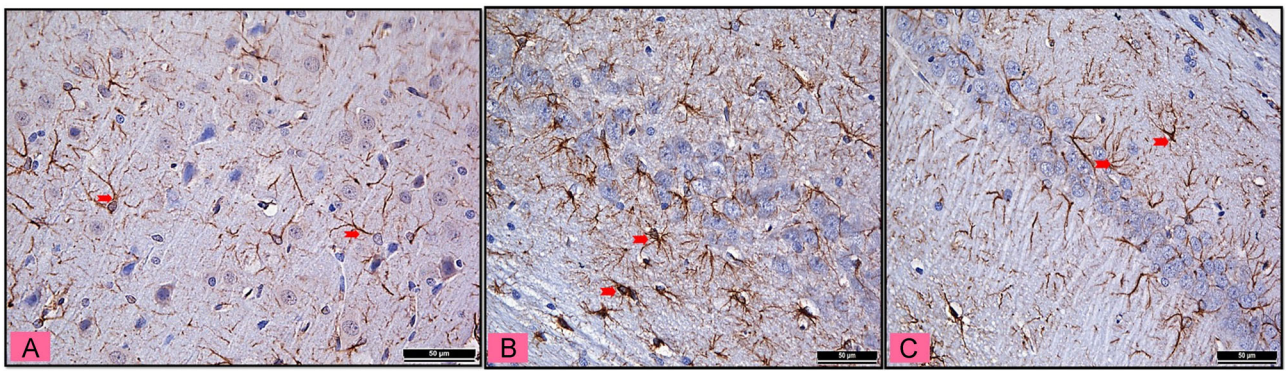

Fig. 8. GFAP immunoreactivity of the RFR Melatonin group (**A**, cortex; **B**, CA3; **C**, CA1). ➡, Astrocytes with GFAP immunoreactivity (immunoperoxidase-hematoxylin ×400). GFAP = glial fibrillary acidic protein; RFR = radiofrequency radiation.

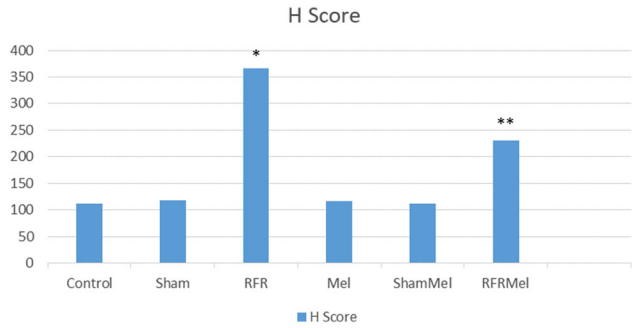

Fig. 9. Mean values of H-score. *Significantly different from Control, Sham, and RFR Melatonin groups ($P < 0.05$). **Significantly different from Control, RFR, Melatonin, and Sham Melatonin groups ($P < 0.05$).

melatonin and sham melatonin groups ($P < 0.05$) (Fig. 13).

DISCUSSION

Mobile phones are a very popular source of RFR and people keep them close to their bodies even while sleeping. Therefore, they are becoming more and more dangerous to human health. LTE (long-term evolution), a type of 4 G (fourth generation) technology, is a telecommunication network and provides high-speed communication [Varshney, 2012]. 2,600 MHz is one of the spectrum bands of LTE. In the present study, exposure to 2,600 MHz RFR for 30 days (30 min/day) decreased the antioxidant parameters and increased the oxidative parameters in the brain tissue of male rats. Also, RFR exposure caused structural changes and increased apoptosis and DNA damage in brain tissue. It was also observed that exogenous melatonin significantly reduced these effects.

The mechanism under the biological effects of RFR is still not clear today. It is thought that RFR interaction with tissue occurs mainly with two mechanisms: thermal and nonthermal. An increase in temperature of the tissue because of RFR is a simple definition of thermal interaction. Secondary to temperature increase, tissue damage may occur, and this can cause adverse health effects. When limit values are stated by the International Commission on Non-Ionizing Radiation Protection (ICNIRP) regarding RFR exposure, RFR is assumed to be thermally effective. However, studies have shown that RFR exposure might cause biological effects at a non-thermal level. This study examined the effects of RFR at nonthermal levels according to ICNIRP limits

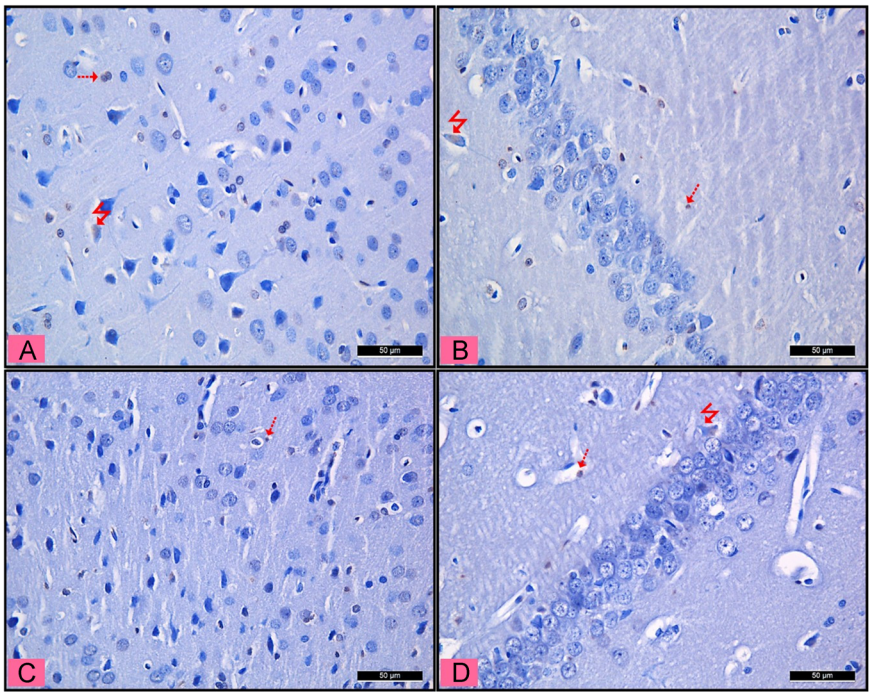

Fig. 10. TUNEL findings of the Control and Sham Control groups. Control (**A**, Cortex; **B**, Hippocampus), Sham Control (**C**, Cortex; **D**, Hippocampus). ↯, TUNEL-positive neurons; ⇢, TUNEL-positive neuroglia cells (TUNEL-hematoxylin ×400). TUNEL = terminal deoxynucleotidyl transferase (TdT)-mediated dUTP nick-end labeling.

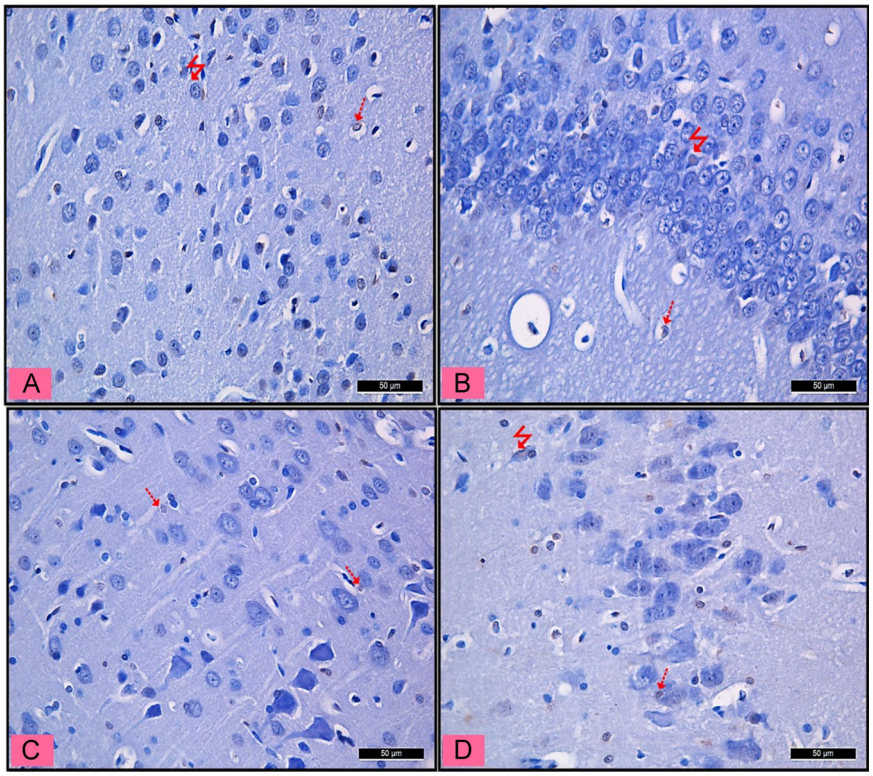

Fig. 11. TUNEL findings of the Sham Melatonin and Melatonin groups. Sham Melatonin (**A**, Cortex; **B**, Hippocampus), Melatonin (**C**, cortex; **D**, Hippocampus). ↯, TUNEL-positive neurons; ⇢, TUNEL-positive neuroglia cells (TUNEL-hematoxylin ×400). TUNEL = terminal deoxynucleotidyl transferase (TdT)-mediated dUTP nick-end labeling.

[ICNIRP, 2010]. Our study showed that RFR could cause harmful effects in brain tissue at nonthermal levels.

Oxidative stress is the most confirmed effect of RFR. Yakymenko et al. [2016] analyzed studies about oxidative stress and low-intensity RFR. They stated that 93 out of 100 studies showed that low-intensity RFR exposure caused oxidative damage in biological organisms. Oxidative stress has an active role in disease pathophysiology. Oxidative damage in brain tissue can cause neurodegeneration. Post-mortem studies have demonstrated increased ROS levels in affected brain tissue areas of individuals with neurodegenerative diseases (Parkinson's disease, Alzheimer's disease [AD], Amyotrophe Lateralsklerose) [Andersen, 2004]. Oxidative stress occurs as a natural result of aging and accelerates aging. Since RFR exposure causes oxidative stress, it suggests that RFR may also have an effect on aging as well as the onset of age-related diseases (AD, atherosclerosis, cardiovascular diseases, cancer) at an earlier age. The current study revealed that exposure of 2600 MHz RFR for 30 days (30 min/day, 5 days/week) caused oxidative changes in rat brain tissue. Similar observations were found by some researchers; Motawi et al. [2014] found that 900 MHz RFR exposure (60 days, 2 h/day, SAR: 1.13 W/kg) induced apoptosis and caused oxidative changes and neuronal damage. Sharma et al. [2019] demonstrated that 2,100 MHz RFR (3 weeks, 5 days/week, 4 h/day, SAR = 0.445 W/kg) exposure induced oxidative stress, caused degeneration in brain tissue, and affected the cognitive functions of rats. Kamali et al. [2018] pointed out that 2.45 GHz RFR (Wi-Fi) exposure (10 weeks, 24 h/day) decreased the activity of some antioxidant enzymes (CAT, GSH-Px, SOD), but GSH and TBARS levels were not affected by the exposure. Chauhan et al. [2017] showed that 2.45 GHz RFR exposure (35 days, 2 h/day, 0.2 mW/cm^2) increased lipid peroxidation in some tissues (brain, liver, and spleen) of rats. However, there are also studies reporting that RFR exposure had no oxidative effect [Demirel et al., 2012; Hong et al., 2012].

RFR-induced oxidative damage can be reduced by using antioxidants. Bilgici et al. [2013] found that 900 MHz RF exposure (3 weeks, 1 h/day, SAR 1.08 W/kg) increased lipid and protein oxidation,

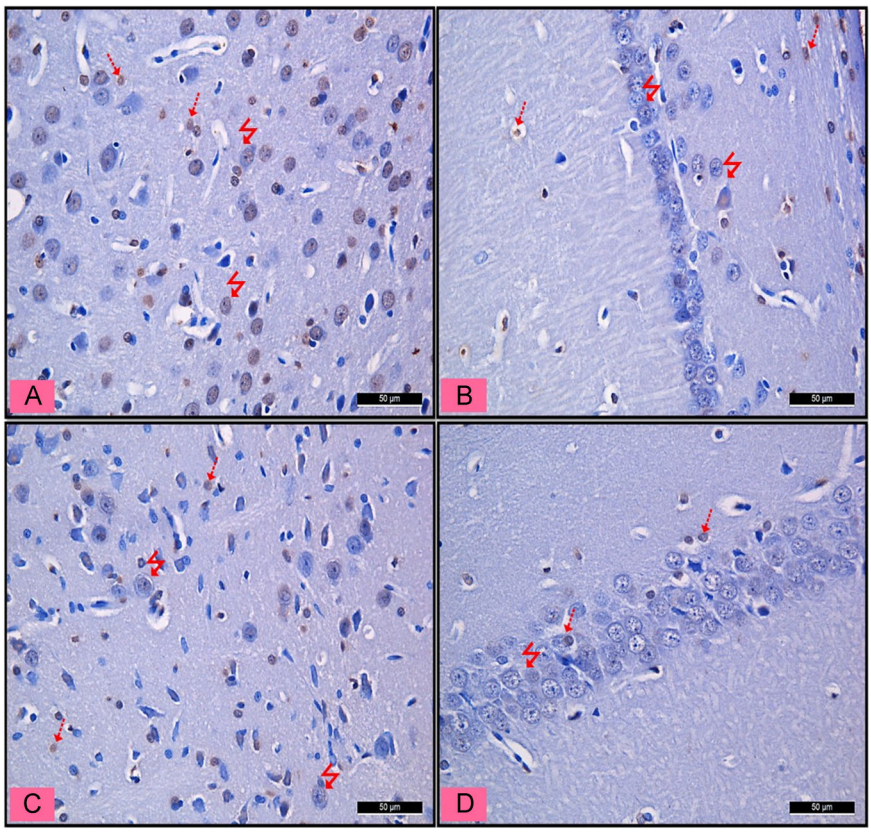

Fig. 12. TUNEL findings of the RFR and RFR Melatonin groups. RFR (**A**, cortex; **B**, Hippocampus), RFR Melatonin (**C**, Cortex; **D**, Hippocampus). ↯, TUNEL-positive neurons; ⇢, TUNEL-positive neuroglia cells (TUNEL-hematoxylin ×400). TUNEL = terminal deoxynucleotidyl transferase (TdT) mediated dUTP nick end labeling.

and garlic powder had a protective effect against oxidative stress secondary to RFR in the brain tissue of rats. Köylü et al. [2006] also showed that 900 MHz RFR exposure (2 weeks, 5 days/week, 30 min/day) caused an increase in lipid peroxidation in the hippocampus and brain tissue of rats. They also reported that in the hippocampus, lipid peroxidation was reduced by melatonin treatment (100 μg/kg, sc, before RFR exposure), but the cortex of the brain tissue was not affected by melatonin treatment. Melatonin had direct free radical scavenging activity and influenced antioxidant enzyme activity [Rodriguez et al., 2004]. Also, melatonin can pass through barriers, such as the blood-brain barrier [Hardeland, 2009]. Therefore, it can be more protective in brain tissue than other antioxidants. Thus, we preferred melatonin as an antioxidant agent in our study. In our daily life, we are exposed to RFR all day long. Since we aimed to observe the effect of melatonin taken at night as a protector for RFR, we carried out melatonin injection daily at 5 pm after RFR exposure.

Some studies demonstrated that RFR exposure affected melatonin release. This could be one of the reasons for oxidative damage secondary to RFR. Burch et al. [2002] showed that long-term (>25 min/day) cell phone use might cause a decrease in melatonin production. Qin et al. [2012] found that 1,800 MHz RF exposure (32 days, 2 h/day) disrupted melatonin and testosterone circadian rhythms, and melatonin was more vulnerable to RFR exposure. Kesari et al. [2011] showed that 900 MHz RFR exposure (45 days, 2 h/day) increased ROS production and decreased GSH-Px and SOD levels in rat brain tissue and melatonin level. In our study, exogenous melatonin reduced RFR adverse effects. One potential explanation for this result could be the decrease of melatonin level because of RFR exposure.

Chauhan et al. [2017] revealed that RFR exposure caused histological alterations in the brain, liver, testis, kidney, and spleen tissues. They found that RFR exposure led to a reduction in pyramidal cells and neuronal degeneration. Koç et al. [2014] showed that 900 MHz RFR exposure during pregnancy caused

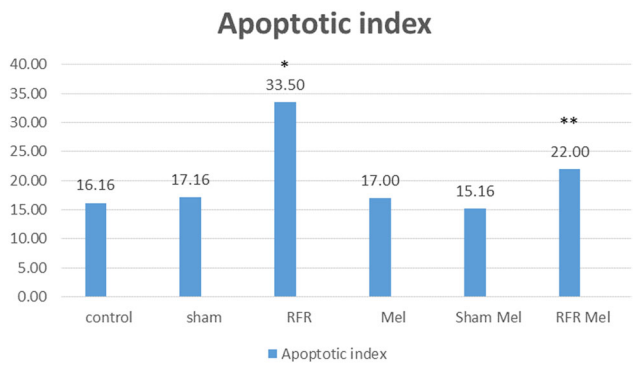

Fig. 13. Mean values of the apoptotic index. *Significantly different from Control, Sham groups ($P < 0.005$). **Significantly different from RFR, Melatonin, and Sham Melatonin groups ($P < 0.05$). RFR = radiofrequency radiation.

neuronal damage in the hippocampus of male offspring, and this damage could be reduced with omega 3 or melatonin. In conjunction with these studies, our study determined that RFR caused structural degeneration in the brain cortex, especially in the hippocampus CA3 region, and caused the loss of neurons and neuroglia cells. In the present study, neurons were observed with abnormal morphology in RFR exposure groups. Apoptotic neurons, a decrease in neuron count, dilated vessels, and edema around neuroglial cells were also seen in RFR exposure groups. Also, melatonin treatment diminished structural degeneration. However, RFR secondary apoptosis could not be completely prevented with melatonin.

The expression of GFAP can be induced by neurodegenerative processes. Increased GFAP levels were shown in patients with AD and dementia [Kashon et al., 2004]. Hausmann et al. [2000] observed the increase of GFAP staining cells after brain injury. In our study, GFAP immunoreactivity was found significantly higher in the RFR group than cage-control, sham, and RFR melatonin groups. These results were confirmed with the H-score analysis. H-score values of the RFR group were considerably higher than cage-control, sham, and RFR melatonin groups. Melatonin diminished the GFAP immunoreactivity density and H-score values.

TUNEL staining is a method that enables the detection of DNA damage occurring in the final stage of apoptosis [Hirose et al., 2006]. In the current study, the number of TUNEL-positive cells increased in RFR groups. We found that melatonin administration decreased the number of TUNEL-positive cells. Based on these findings, it can be inferred that DNA damage induced by RFR exposure may be reduced by using melatonin. Contrary to our results, Akdag et al. [2016] showed that 2.45 GHz RFR exposure for 1 year increased DNA damage (with the comet assay method) in the brain, liver, kidney, skin, and testicular tissues of rats; however, this increase was statistically significant only in testicular tissue, and the increase in brain tissue was not significant. On the contrary, Kesari et al. [2010] stated that 2.45 GHz RFR exposure (35 days, 2 h/day, power density: 0.34 mW/cm^2, SAR: 0.11 W/kg) increased the DNA damage of Wistar rats' brain tissue.

In our study, apoptosis was seen in both neuron and neuroglial cells in the cortex but was mostly in neuroglial cells in the hippocampus. Since nerve cells do not have regeneration capacity, apoptosis occurring in neurons can lead to neurodegenerative diseases. On the contrary, apoptosis of glial cells carries a risk of malignancy [Phillips et al., 2009]. By considering our findings, it can be said that RFR may be a risk factor for both neurodegenerative diseases and brain tumors. In this present study, exposure was performed 5 days a week, so observed effects might be at a more moderate level. As even short-term exposure (30 min per day) caused these effects, it could be important to consider the effects of RFR.

CONCLUSION

In this study, RFR caused oxidative stress by increasing oxidative parameters and by decreasing antioxidant parameters in the brain tissue. Also, exogenous melatonin treatment significantly decreased the oxidative effects of RFR exposure. RFR caused apoptosis and structural degeneration in the brain tissue, melatonin administration had played an active role in the elimination of this structural degeneration, and GFAP immunoreactivity and the number of TUNEL-positive neurons approached or returned to normal with melatonin. Therefore, reducing RFR exposure time is one of the precautions that should be taken into consideration. Also, it is important to emphasize that taking exogenous melatonin could be protective.

ETHICAL APPROVAL

The present study had been approved by Gazi University Animal Experiments Local Ethics Committee (G.Ü. ET-17.039).

REFERENCES

Aalto S, Haarala C, Brück A, Sipilä H, Hämäläinen H, Rinne JO. 2006. Mobile phone affects cerebral blood flow in humans. J Cereb Blood Flow Metab 26:885–890.

Abdel-Rassoul G, El-Fateh OA, Salem MA, Michael A, Farahat F, El-Batanouny M, Salem E. 2007. Neurobehavioral effects

among inhabitants around mobile phone base stations. Neurotoxicology 28:434–440.
Akdag MZ, Dasdag S, Canturk F, Karabulut D, Caner Y, Adalier N. 2016. Does prolonged radiofrequency radiation emitted from Wi-Fi devices induce DNA damage in various tissues of rats? J Chem Neuroanat 75:116–122.
Alkis ME, Bilgin HM, Akpolat V, Dasdag S, Yegin K, Yavas MC, Akdag MZ. 2019. Effect of 900-, 1800-, and 2100-MHz radiofrequency radiation on DNA and oxidative stress in brain. Electromagn Biol Med 38:32–47.
Andersen JK. 2004. Oxidative stress in neurodegeneration: Cause or consequence? Nat Med 10:S18–S25.
Baan R, Grosse Y, Lauby-Secretan B, El Ghissassi F, Bouvard V, Benbrahim-Tallaa L, Guha N, Islami F, Galichet L, Straif K. 2011. Carcinogenicity of radiofrequency electromagnetic fields. Lancet Oncol 12:624–626.
Bilgici B, Akar A, Avci B, Tuncel OK. 2013. Effect of 900 MHz radiofrequency radiation on oxidative stress in rat brain and serum. Electromagn Biol Med 32:20–29.
Bothorel B, Barassin S, Saboureau M, Perreau S, Vivien-Roels B, Malan A, Pévet P. 2002. In the rat, exogenous melatonin increases the amplitude of pineal melatonin secretion by a direct action on the circadian clock. Eur J Neurosci 16:1090–1098.
Burch J, Reif J, Noonan C, Ichinose T, Bachand A, Koleber T, Yost M. 2002. Melatonin metabolite excretion among cellular telephone users. Int J Radiat Biol 78:1029–1036.
Chauhan P, Verma H, Sisodia R, Kesari KK. 2017. Microwave radiation (2.45 GHz)-induced oxidative stress: Whole-body exposure effect on histopathology of Wistar rats. Electromagn Biol Med 36:20–30.
Demirel S, Doganay S, Turkoz Y, Dogan Z, Turan B, Firat PGB. 2012. Effects of third generation mobile phone-emitted electromagnetic radiation on oxidative stress parameters in eye tissue and blood of rats. Cutan Ocul Toxicol 31:89–94.
Halliday GM, Cullen KM, Kril JJ, Harding AJ, Harasty J. 1996. Glial fibrillary acidic protein (GFAP) immunohistochemistry in human cortex: A quantitative study using different antisera. Neurosci Lett 209:29–32.
Hardeland R. 2009. Melatonin: Signaling mechanisms of a pleiotropic agent. Biofactors 35:183–192.
Hausmann R, Riess R, Fieguth A, Betz P. 2000. Immunohistochemical investigations on the course of astroglial GFAP expression following human brain injury. Int J Legal Med 113:70–75.
Hirose H, Sakuma N, Kaji N, Suhara T, Sekijima M, Nojima T, Miyakoshi J. 2006. Phosphorylation and gene expression of p53 are not affected in human cells exposed to 2.1425 GHz band CW or W-CDMA modulated radiation allocated to mobile radio base stations. Bioelectromagnetics 27:494–504.
Hong MN, Kim BC, Ko YG, Lee YS, Hong SC, Kim T, Pack JK, Choi HD, Kim N, Lee JS. 2012. Effects of 837 and 1950 MHz radiofrequency radiation exposure alone or combined on oxidative stress in MCF10A cells. Bioelectromagnetics 33:604–611.
John T, Liu G, Tsao M. 2009. Overview of molecular testing in non-small-cell lung cancer: Mutational analysis, gene copy number, protein expression and other biomarkers of EGFR for the prediction of response to tyrosine kinase inhibitors. Oncogene 28:S14–S23.
Joubert V, Leveque P, Cueille M, Bourthoumieu S, Yardin C. 2007. No apoptosis is induced in rat cortical neurons exposed to GSM phone fields. Bioelectromagnetics 28:115–121.
Kamali K, Taravati A, Sayyadi S, zahra Gharib F, Maftoon H. 2018. Evidence of oxidative stress after continuous exposure to Wi-Fi radiation in rat model. Environ Sci Pollut Res 25:35396–35403.
Kashon ML, Ross GW, O'Callaghan JP, Miller DB, Petrovitch H, Burchfiel CM, Sharp DS, Markesbery WR, Davis DG, Hardman J. 2004. Associations of cortical astrogliosis with cognitive performance and dementia status. J Alzheimer's Dis 6:595–604.
Kerman M, Senol N. 2012. Oxidative stress in hippocampus induced by 900 MHz electromagnetic field emitting mobile phone: Protection by melatonin. Biomed Res 23:147–151.
Kesari KK, Behari J, Kumar S. 2010. Mutagenic response of 2.45 GHz radiation exposure on rat brain. Int J Radiat Biol 86:334–343.
Kesari KK, Kumar S, Behari J. 2011. 900-MHz microwave radiation promotes oxidation in rat brain. Electromagn Biol Med 30:219–234.
Koç GE, Kaplan S, Altun G, Gümüş H, Deniz ÖG, Aydın I, Önger ME, Altunkaynak BZ. 2014. Neuroprotective effect of melatonin and omega-3 on the hippocampus of rat that prenatally exposed to 900 mhz electromagnetic fields. Deneysel ve Klinik Tıp Dergisi 31:130.
Köylü H, Mollaoglu H, Ozguner F, Nazýroölu M, Delibap N. 2006. Melatonin modulates 900 Mhz microwave-induced lipid peroxidation changes in rat brain. Toxicol Ind Health 22:211–216.
Lustenberger C, Murbach M, Dürr R, Schmid MR, Kuster N, Achermann P, Huber R. 2013. Stimulation of the brain with radiofrequency electromagnetic field pulses affects sleep-dependent performance improvement. Brain Stimul 6:805–811.
Megha K, Deshmukh PS, Banerjee BD, Tripathi AK, Ahmed R, Abegaonkar MP. 2015. Low intensity microwave radiation induced oxidative stress, inflammatory response and DNA damage in rat brain. Neurotoxicology 51:158–165.
Middeldorp J, Hol E. 2011. GFAP in health and disease. Prog Neurobiol 93:421–443.
Motawi TK, Darwish HA, Moustafa YM, Labib MM. 2014. Biochemical modifications and neuronal damage in brain of young and adult rats after long-term exposure to mobile phone radiations. Cell Biochem Biophys 70:845–855.
Pan M, Song YL, Xu JM, Gan HZ. 2006. Melatonin ameliorates nonalcoholic fatty liver induced by high-fat diet in rats. J Pineal Res 41:79–84.
Phillips JL, Singh NP, Lai H. 2009. Electromagnetic fields and DNA damage. Pathophysiology 16:79–88.
Icnirp. 2010. Guidelines for limiting exposure to time-varying electric and magnetic fields (1 Hz to 100 kHz). Health Phys 99:818–836.
Qin F, Zhang J, Cao H, Yi C, Li JX, Nie J, Chen LL, Wang J, Tong J. 2012. Effects of 1800-MHz radiofrequency fields on circadian rhythm of plasma melatonin and testosterone in male rats. J Toxicol Environ Health Part A 75:1120–1128.
Reiter RJ, Tan DX, Galano A. 2014. Melatonin: exceeding expectations. Physiology 29:325–333.
Rodriguez C, Mayo JC, Sainz RM, Antolín I, Herrera F, Martín V, Reiter RJ. 2004. Regulation of antioxidant enzymes: a significant role for melatonin. J Pineal Res 36:1–9.
Sakuma N, Komatsubara Y, Takeda H, Hirose H, Sekijima M, Nojima T, Miyakoshi J. 2006. DNA strand breaks are not induced in human cells exposed to 2.1425 GHz band CW and W-CDMA modulated radiofrequency fields allocated to mobile radio base stations. Bioelectromagnetics 27:51–57.

Salford LG, Brun AE, Eberhardt JL, Malmgren L, Persson BR. 2003. Nerve cell damage in mammalian brain after exposure to microwaves from GSM mobile phones. Environ Health Perspect 111:881–883.

Schmidt-Kastner R, Wietasch K, Weigel H, Eysel U. 1993. Immunohistochemical staining for glial fibrillary acidic protein (GFAP) after deafferentation or ischemic infarction in rat visual system: features of reactive and damaged astrocytes. Int J Dev Neurosci 11:157–174.

Sharma R, Sharma S, Shrivastava S, Singhal PK, Shukla S. 2019. Mobile phone induced cognitive and neurochemical consequences. J Chem Neuroanat 102:101684.

Sharma R, Masaki J, Agarwal A. 2013. Sperm DNA fragmentation analysis using the TUNEL assay. Methods Mol Biol 927:121–36.

Sirav B, Seyhan N. 2016. Effects of GSM modulated radiofrequency electromagnetic radiation on permeability of blood–brain barrier in male & female rats. J Chem Neuroanat 75:123–127.

Varshney U. 2012. 4G wireless networks. IT Professional 14:34–39.

Yakymenko I, Tsybulin O, Sidorik E, Henshel D, Kyrylenko O, Kyrylenko S. 2016. Oxidative mechanisms of biological activity of low-intensity radiofrequency radiation. Electromagn Biol Med 35:186–202.